

SPEED DISTRIBUTION ANALYSIS IN A LUBRICATING FLUID NEAR A IDEAL ROUGOSITY

Fomin Michaela Vasilache¹

¹Department of Mechanics and Technologies, Ștefan cel Mare University of Suceava, ROMÂNIA

¹fomin_michaela@yahoo.com

Abstract: Scuffing as a final result of the shearing stress limit exceeding stress occurring in the fluid, being possible through the thinning of the lubricant film until direct contact between bodies. Rugosity introduces tangential stress at the limit, this being additional in the lubricant film. The paper studies the adjacent zone to rugosity, in terms of the speed distribution.

Keywords: speed, rugosity, shearing stress limit;

1. Introduction

This paper proposes an analysis of speed distribution in a lubricating fluid in the vicinity of a rugosity. In order to facilitate mathematical calculations we proposed a triangular rugosity model, which is idealized through the fact that it is not connected by a radius at the top. The model proposes the analysis in terms of scuffing occurrence conditions and not from the perspective of lubricant flow analysis.

The model of ideal rugosity geometrically consists of two intersecting planes, so it can be considered two symmetrical and equal, classical hydrodynamic "pads". We also consider that the fluid is Newtonian with plastic limit.

If the fluid motion is considered laminar, therefore no turbulence occurs, this model can only exist if we take into consideration the appearance of shear stress limit in the vicinity of the rugosity, in order to level the high discontinuity. Therefore we propose a viscoplastic fluid lubrication models, taking into account the research conducted by Huang & Wen, [1], Diaconescu, [2] and Balan [3] based on the relation:

$\tau_l = \tau_{l0} + (1)$ where τ_l is the shearing stress limit depending on pressure, τ_{l0} is the shearing stress limit under atmospheric pressure and ϵ is a dimensionless coefficient.

A newtonian viscoplastic fluid behaves as a rigid on low shearing stress, but it flows as a viscous fluid at high shear values. Given that simultaneous with the growth of the product

the shear stresses increase, according to the relation:

$$\tau = \eta_e \dot{\gamma} = \eta_e \quad (2)$$

(where, η_e is the effective lubricant viscosity, u the speed in the considered point and $\dot{\gamma}$ is the shearing speed, which is equal to the speed gradient on the flow plane's normal direction), the maximum value can be achieved only on one of the surfaces. Once maximal shearing stress is reached, increasing viscosity or decreasing film thickness variations can generate the emergence of a sliding contact between the fluid and the contact surface [4].

The issue of speed distribution observation arises in the plastic shearing areas for the proposed model (figure 1). Lubricant's

speed in a given point is $u = u(x, z)$, being oriented to the right.

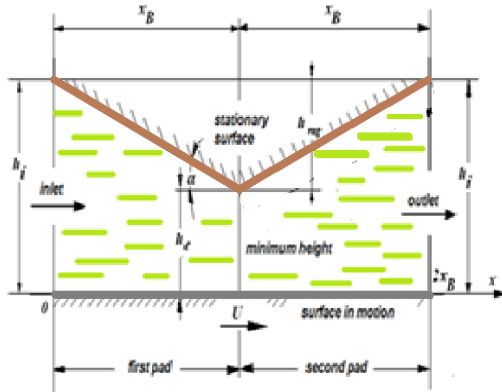


Figure 1. Geometry of a triangular asperity[5]

From the equilibrium equation of an elementary volume and the constitutive equation, (Newton's relationship) assuming a constant viscosity, it results:

$$\frac{\partial^2 u}{\partial z^2} = \frac{1}{\eta} \tau \quad (3)$$

double integration lead to the following expression:

$$u = \frac{1}{2\eta} \frac{dp}{dx} z^2 + C_1 z + C_2 \quad (4)$$

Where C_1 and C_2 constants can be calculated from the limit conditions:

$$\left\{ \begin{array}{l} \text{for } z=0; u=U \rightarrow C_2 = U \\ \text{for } z=h; u=0 \rightarrow C_1 = -\frac{u}{h} - \frac{1}{\eta} \frac{dp}{dx} \frac{h}{2} \end{array} \right\} \quad (5)$$

By replacing and customizing for each pad, the following expressions for speed distribution are obtained:

$$u_1 = \frac{1}{2\eta} \frac{dp_1}{dx} (z^2 - zh_1) + U \left(1 - \frac{z}{h_1} \right) \quad (6)$$

$$u_2 = \frac{1}{2\eta} \frac{dp_2}{dx} (z^2 - zh_2) + U \left(1 - \frac{z}{h_2} \right) \quad (7)$$

Or for the two pads, speed distribution over the rough surfaces is:

$$u(x, z) = \left\{ \begin{array}{l} u_1(x, z) \text{ for } 0 < x < x_B \\ u_2(x, z) \text{ for } x_B < x < 2x_B \end{array} \right\} \quad (8)$$

Speed distribution graphics were drawn for a specific case, with the following data:

plane speed $U=10$ [m/s],
 pad's length $x_B=0,00025 \times 10^{-3}$ [m],
 asperity's height $h_{rug}=0,0005 \times 10^{-3}$ [m],
 the minimal thickness of the lubricant film $h_e=0,01 \times 10^{-3}$ [m],
 the output (input) thickness $h_i = h_e + h_{rug} = 0,0015 \times 10^{-3}$ [m],

thickness input/output ratio, $a = \frac{h_i}{h_e} = 1,5$

and dynamic viscosity $\eta = 0,15$ [Pas].

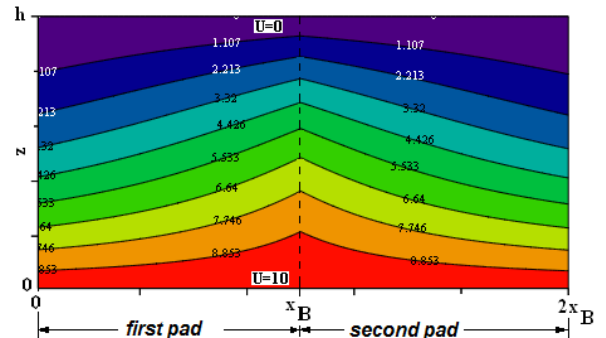


Figure 2. Particular case for the specified values [5].

Speed evolution can be observed from $z=0$ where the speed is 10[m/s] to $z=h$, where speed is 0. Also, approximately parallel fluid lines that have the same speed can be observed (the working hypothesis being that of laminar flow).

After analysing pressure, shear stress, speed and temperature from the vicinity of a triangular rugosity [5], the relevant situations of shear stress limit occurrence can be summarized. Taking into account increasing speed values, the cases in which plastic shearing occur [5] prove to be different from those observed in Diaconescu and Balan models, on account of the second part of the rugosity, where shear stress limit is reached faster.

Case 1

This case is suggested in Figure 3, which as can be seen (in bold line), the shear stress limit is reached on the rugosity surface to the output of the first part of the rugosity (between x_{j1} and x_B) and also on the upper surface at the output of the second part of the rugosity (between x_B and x_{j2}). The three different lubrication zones thus formed (marked in the figure as viscous, viscoplastic and again viscous) are joined off the abscissae x_{j1} and x_{j2} .

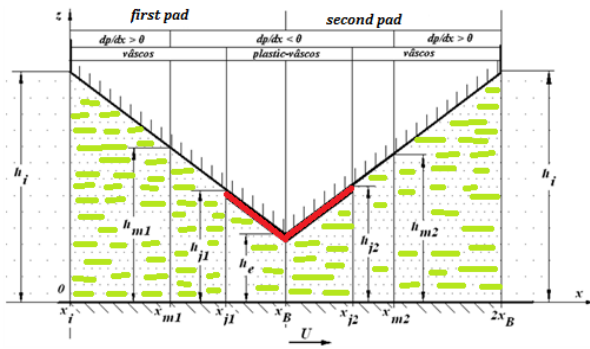


Figure 3 Contact's geometry and shear stress limit distribution – case I

Speed distribution over the rough surface is obtained through relations connection of the four speed distribution relations corresponding to the four areas, as in the system:

$$u(x, z) \begin{cases} u_{v1}(x, z) \text{ for } 0 < x < x_{j1} \\ u_{pv1}(x, z) \text{ for } x_{j1} < x < x_B \\ u_{pv2}(x, z) \text{ for } x_B < x < x_{j2} \\ u_{v2}(x, z) \text{ for } x_{j2} < x < 2x_B \end{cases} \quad (9)$$

Case II

Maintaining constant geometrical and material parameters, with further increasing speed it occurs another case of plastic shear. Plastic shear stress at the plan's limit for the second part of the rugosity intersects the negative shear stress limit in x_{j22} and $2x_B$.

Unlike the previous case, this situation involves plastic shearing also on the plan's surface over the second part of the rugosity of an abscissa, x_{j22} , until the end. Thus five different lubrication zones occur over the

rough surface. The first two areas; viscous, $0 - x_{j1}$ and viscoplastic $x_{j1} - x_B$, corresponding to the first patina are similar to the prior case (first case of plastic shearing).

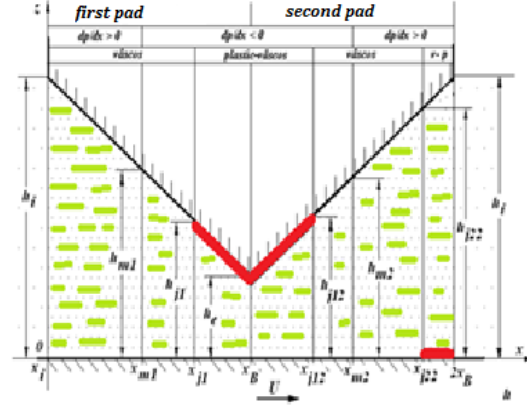


Figure 4. Contact's geometry and shear stress limit distribution – case II

For the second patina the next three areas appear:

1. **viscoplastic**, corresponding to the interval, $x_B - x_{j12}$
2. **newtonian viscous**, corresponding to the interval, $x_{j12} - x_{j22}$; and
3. **viscoplastic** corresponding to the interval $x_{j22} - 2x_B$. Speed distribution for the first two viscous areas (interval $0 - x_{j1}$) and viscoplastic, (interval $x_{j1} - x_B$), corresponding to the first part of the rugosity are similar to the prior case, (plastic shearing in the 1st case).

Over the entire rugosity surface speed distribution is:

$$u(x, z) \begin{cases} u_{v1}(x, z) \text{ for } 0 < x < x_{j1} \\ u_{pv1}(x, z) \text{ for } x_{j1} < x < x_B \\ u_{pv2}(x, z) \text{ for } x_B < x < x_{j12} \\ u_{v2}(x, z) \text{ for } x_{j12} < x < 2x_B \\ u_{vp2}(x, z) \text{ for } x_{j22} < x < 2x_B \end{cases} \quad (10)$$

$$u(x, z) \begin{cases} u_{v1}(x, z) \text{ for } 0 < x < x_{j1} \\ u_{pv1}(x, z) \text{ for } x_{j1} < x < x_B \\ u_{pv2}(x, z) \text{ for } x_B < x < x_{j2} \\ u_{v2}(x, z) \text{ for } x_{j2} < x < 2x_B \end{cases} \quad (11)$$

For the same geometrical and material parameters, similar to the prior case (first case

of plastic shearing) solutions for the second case for speeds higher than $U = 17,84$ [m/s] up to $U = 18,04$ [m/s].

Case III . Speed distribution

For a higher speed, viscoplastic shearing solutions for the second situation are not obtained, this situation determining the third case of viscoplastic shearing, which is similar to the precedent case, but where plastic shearing in a plane's surface input within the range of the first part of the rugosity.

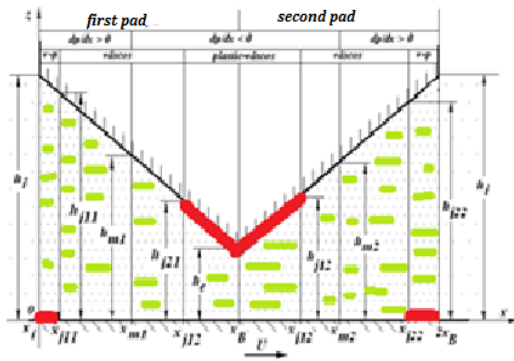


Figure 5. Contact's geometry and shear stress limit distribution – case III

The evolution of the pressure distribution in transition to this case reveals three areas for the first part of the rugosity and three different reaction zones for the second one. From a quality perspective the areas are symmetrical against a perpendicular passing through the abscissa x_B and will have the same types of equations, only the followed occurring effects interval size differ. The abscissae corresponding to maxim (x_{m1}) and minim (x_{m2}) pressure is situated in the viscous areas. Due to the complexity of this case, where six different areas occur, the methodology for determining speed distribution is dealt with in detail.

For the first part of the rugosity, the first zone between $0 - x_{j11}$, where lubricant's behaviour is viscoplastic speed distribution is obtained through pressure distribution [5]

$$p_{vp1} = \left[\frac{\tau_{10}}{\beta} - \frac{3\eta U}{3\beta + 4k_1} \frac{h_m}{h_i^2} \right] \left(\frac{h_1}{h_i} \right)^{\frac{3\beta}{2k_1}} - \frac{\tau_{10}}{\beta} + \frac{3\eta U}{3\beta + 4k_1} \frac{h_m}{h_i^2}$$

and pressure gradient,

$$\frac{dp_{vp1}}{dh_1} = \left[\frac{3\tau_{10}}{2k_1 h_i} - \frac{9\beta}{2k(3\beta + 4k_1)} \frac{\eta U h_m}{h_i^3} \right] \left(\frac{h_1}{h_i} \right)^{\frac{3\beta - 2k_1}{2k_1}} - \frac{\tau_{10}}{\beta} + \frac{6\eta U}{3\beta + 4k_1} \frac{h_m}{h_i^3}$$

In the relation

$$U_{GP>0} = \frac{1}{2\eta} \frac{dp}{dx} (z^2 - h^2) - \frac{(\tau_{10} + \beta p)}{\eta} (h - z)$$

where plastic shearing is reached on the lower surface and pressure gradient is positive. It is obtained:

$$U_{vp1} = \frac{1}{\eta} \frac{dp_{vp1}}{dh_1} (z^2 - h^2) - \frac{(\tau_{10} + \beta p_{vp1})}{\eta} (h_1 - z) \quad (12)$$

For the first part of the rugosity' second area, in the range $x_{j11} - x_{j21}$, where the lubricant is newtonian viscous it is obtained through the substitution of the pressure gradient corresponding to this area in the speed distribution relation in the case of the absence of plastic shearing, therefore obtaining:

$$U_{v1}(x, z) = \frac{1}{2\eta} \frac{dp_{v1}}{dh_1} (z^2 - zh_1) + U \left(1 - \frac{z}{h_1} \right) \quad (13)$$

For the last area of the second part of the rugosity, in the range $x_{j21} - x_B$ (the area in which plastic shearing occurs on the upper surface and the gradient is negative) it is obtained:

$$u_{pv1} = \frac{1}{\eta} \frac{dp_{pv1}}{dh_1} \left(\frac{z^2}{2} - h_1 z \right) - \frac{(\tau_{10} + \beta p_{pv1})}{\eta} z + U \quad (14)$$

For the second part of the rugosity, the relations are similar to those in the previous case and we just remind them here:

For the second part of the rugosity's first area (interval $x_B - x_{j12}$)

$$u_{pv2} = \frac{1}{\eta} \frac{dp_{pv2}}{dh_2} \left(\frac{z^2}{2} - h_2 z \right) - \frac{(\tau_{10} + \beta p_{pv2})}{\eta} z + U \quad (15)$$

For the second part of the rugosity's second area (interval $x_{j12} - x_{j22}$)

$$u_{v2}(x, z) = \frac{1}{2\eta} \frac{dp_{pv2}}{dh_2} (z^2 - zh_2) + U \left(1 - \frac{z}{h_2} \right) \quad (16)$$

For the second part of the rugosity's third area (interval $x_{j22} - 2x_B$)

$$u_{vp2} = \frac{1}{\eta} \frac{dp_{pv2}}{dh_2} (z^2 - h_2^2) - \frac{(\tau_{10} + \beta p_{pv2})}{\eta} (h_2 - z) \quad (17)$$

By merging all zones along the rough area we get the following speed distribution:

$$u(x,z) \begin{cases} u_{vp1}(x,z) \text{ for } 0 < x < x_{j11} \\ u_{v1}(x,z) \text{ for } x_{j11} < x < x_{j21} \\ u_{pv1}(x,z) \text{ for } x_{j21} < x < x_B \\ u_{pv2}(x,z) \text{ for } x_B < x < x_{j12} \\ u_{v2}(x,z) \text{ for } x_{j12} < x < x_{j22} \\ u_{vp2}(x,z) \text{ for } x_{j22} < x < 2x_B \end{cases} \quad (18)$$

For the geometrical and material parameters, the same as in the previous cases (first and second case of plastic shearing) for the third case we obtain speeds higher than $U=18,04$ [m/s] up to $U=18,046$ [m/s]. It is a very small range for speeds, given the selection method, inferred for the first part of the rugosity and rather logically assumed for the second part of the rugosity (according to Diaconescu's third model [2]). Plan's speed is $U= 18,046$ [m/s], this being the limit of passing to the next plastic shearing case.

Speed distribution case IV

For plan's higher speeds for the third case plastic shearing solutions are no longer achieved for systems' connections conditions of the third case of plastic shearing. Therefore we should pass to the fourth case of plastic shearing. This is considered similar to the previous one, only for the second part of the rugosity plastic shearing areas merge over the abscissa corresponding to maximum pressure, according to the suggested model (Figure 7).

So, for the first part of the rugosity, this situation is identical to the previous case and for the second part of the rugosity a Diaconescu's total shearing over the entire pad is taken into consideration, [2]. There are three cases. There are three zones for the first part of the rugosity, the same as in the previous case and two different reaction areas for the second part of the rugosity, just like a Diaconescu model but with vacuum rather than pressure. It is also assumed that the abscissa

corresponding to the maximum pressure (x_{m1}) for the first part of the rugosity is in the viscous area and the abscissa corresponding to the minimum pressure (x_{m2}) is between the two zones, plastic-viscous $x_B - x_{j2}$ and viscoplastic $x_{j2}-2x_B$.

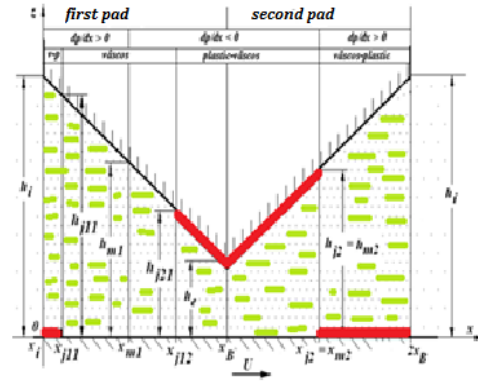


Figure 7. Contact's geometry and shear stress limit distribution – case IV

After solving system's connection conditions for the second part of the rugosity, $U_f=24,544$ [m/s] speed is achieved, for which speed plastic shearing occurs throughout the entire pad, according to Diaconescu's fourth model [2]. With this speed, for the first connection system, viable solutions necessary for the first part of the rugosity are not achieved. At the same time, the heights corresponding to the minimum and maximum pressures resulting from the Mathcad numerical solving of the connection conditions are no longer equal $h_{m1} = 1,375 \times 10^{-5}$; $h_{m2} = 1,474 \times 10^{-5}$. Therefore this case can exist only for the proposed model, of two pads but not in terms of rugosity.

Conclusions

High pressure and low shearing speed – conditions for an elastic lubricant behaviour– may lead to lubricant's solid plastic manifestation on an increasing speed.

Considering a newtonian viscous model, in terms of asperity values similar to the proposed model, leads to higher tangential stress than in the case of viscoplastic fluids (fluids that have a shearing stress limit).

In terms of distribution speed, the correlation of reaching limit shearing stress in the proposed model induces the idea that increasing speed rushes scuffing.

References

- [1] Huang P., Wen S.Z., A New Model of Visco-Plastic Fluid Lubrication for Sliding Problems, Acta tribologica, Vol. 2, p. 23-30, Suceava, 1994.
- [2] Diaconescu E., 1996, Shear stress of lubricant film, ROTRIB TCMM-18, pp. 70-79., Suceava, 1996.
- [3] Balan M., Theoretical introduction concerning shear stress of lubricant film, Paper in the PhD program, p.81, Suceava, 2000.
- [4] Musca I., The behaviour of oil under pressure, Didactic and Pedagogic Publishing House , p.148, Suceava, 2004.
- [5] Fomin M., Preliminary theoretical contributions relating to the phenomenon of scuffing, Paper in the PhD program , p.89, Suceava, 2011.